Elsevier Editorial System(tm) for
Geomechanics for Energy and the Environment
Manuscript Draft

Manuscript Number:

Title: Effect of temperature induced excess porewater pressures on the shaft bearing capacity of geothermal piles

Article Type: SI:Selected papers SEG2015

Keywords: piles, geothermal, bearing capacity, energy

Corresponding Author: Dr. Raul Fuentes, EngD, MSc, Ingeniero

Corresponding Author's Institution: University of Leeds

First Author: Raul Fuentes, EngD, MSc, Ingeniero

Order of Authors: Raul Fuentes, EngD, MSc, Ingeniero; Nuria Pinyol; Eduardo Alonso

Abstract: Changes in temperature in clays of low permeability typically induce excess porewater pressures. In the context of geothermal piles this effect has typically been overlooked since most installations have occurred in soils with higher values of permeability. A parametric study is presented that solves the governing differential equations one dimensionally in a pile to study the influence of the various parameters: permeability and soil compressibility. A new shaft resistance reduction ratio has been also defined to illustrate the loss of bearing capacity. The study shows that when the value of permeability is 1E-11 m/s or lower, combined with a soil compressibility in excess of 2E10 Pa, the excess porewater pressures can be comparable to typical mobilised shaft resistances. The solution applied to the case of the Lambeth College, London, also provides a plausible explanation to the observed loss of shaft friction of the tested pile.

Figure 1

Click here to download high resolution image

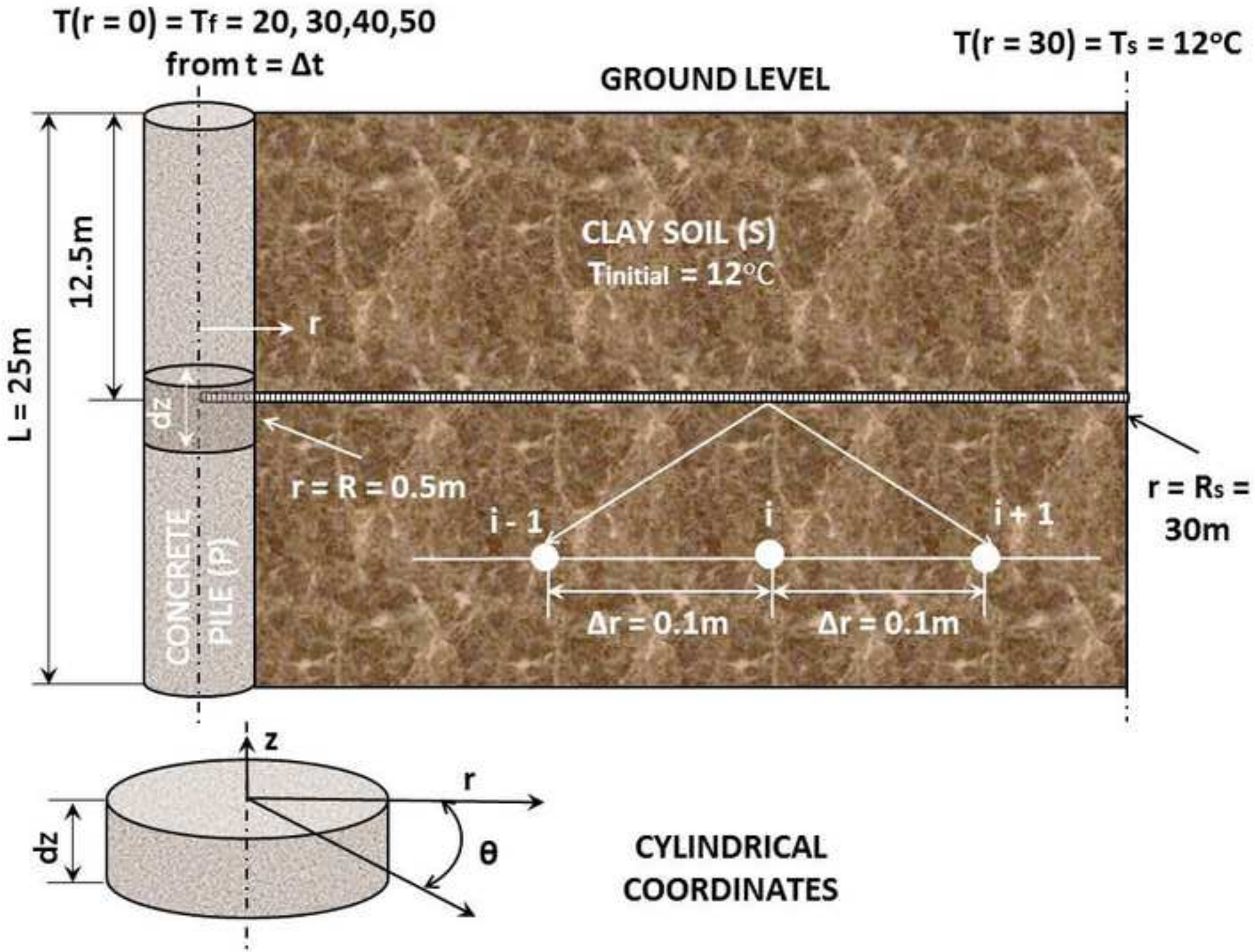

Figure 2

Click here to download high resolution image

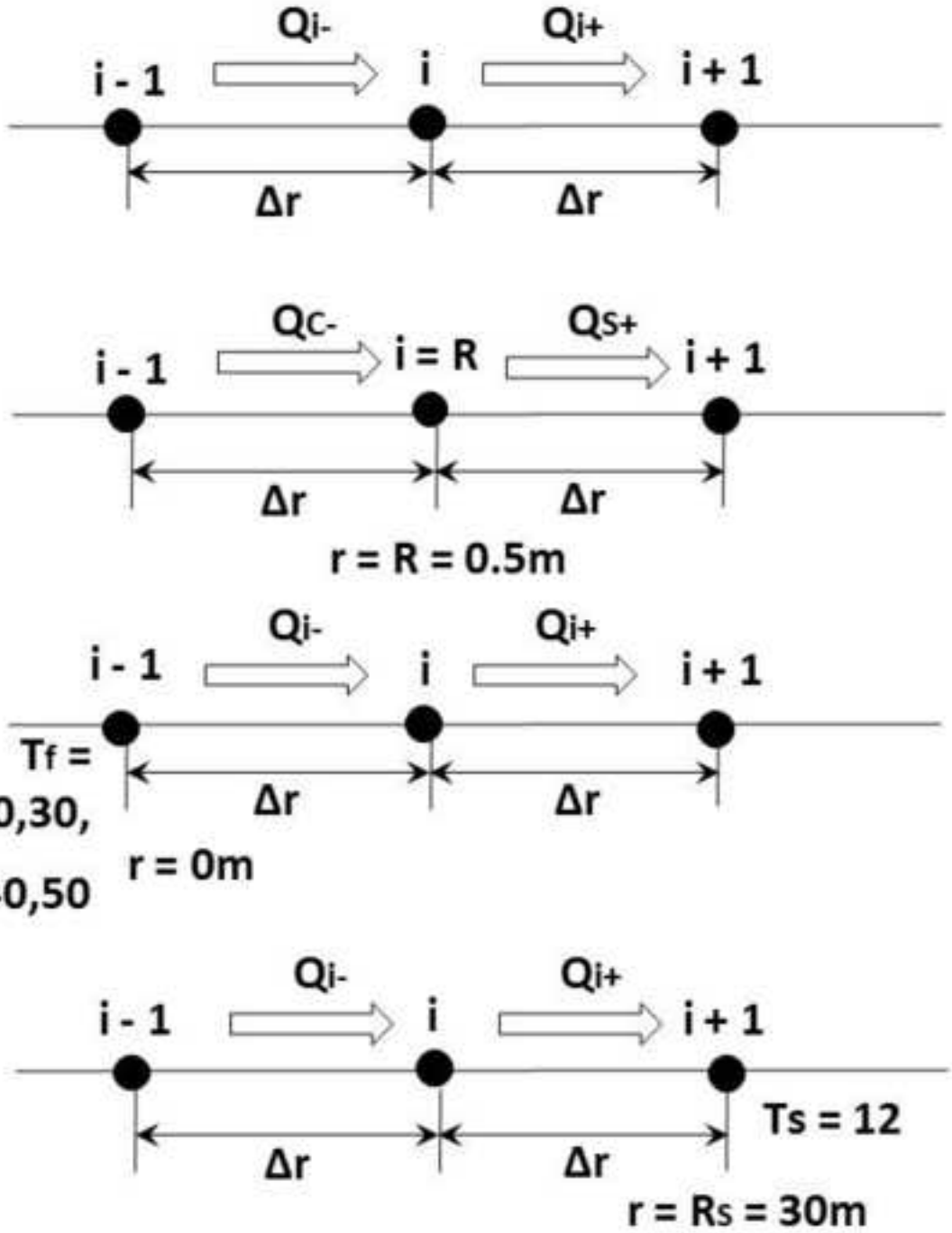

Title: Effect of temperature induced excess porewater pressures on the shaft bearing capacity of geothermal piles

Corresponding author: Raul Fuentes, EUR ING, MSc, EngD, Ing., Civiling. MIDA, CEng MICE

Affiliation: University of Leeds

Address: School of Civil Engineering, University of Leeds, Leeds, LS2 9JT, UK

Telephone: (+44) 0113 343 2282

Email: r.fuentes@leeds.ac.uk

Other authors: Nuria Pinyol, Eduardo Alonso

Affiliation: Universidad Politecnica de Catalunya

Address: Department of Geotechnical Engineering and Geo-Sciences, c/ Jordi Girona, 1-3, Building D2, Barcelona, 08034, Spain

Emails: nuria.pinyol@upc.edu , eduardo.alonso@upc.edu

Abstract

Changes in temperature in clays of low permeability typically induce excess porewater pressures. In the context of geothermal piles this effect has typically been overlooked since most installations have occurred in soils with higher values of permeability. A parametric study is presented that solves the governing differential equations one dimensionally in a pile to study the influence of the various parameters: permeability and soil compressibility. A new shaft resistance reduction ratio has been also defined to illustrate the loss of bearing capacity. The study shows that when the value of permeability is 1E-11 m/s or lower, combined with a soil compressibility in excess of 2E10 Pa, the excess porewater pressures can be comparable to typical mobilised shaft resistances. The solution applied to the case of the Lambeth College, London, also provides a plausible explanation to the observed loss of shaft friction of the tested pile.

Keywords: *piles, geothermal, bearing capacity*

Introduction

Soils with low permeability can experience substantial increases in their pore water pressures as a consequence of temperature rises (e.g. Laloui, 2001; Vardoulakis, 2002; Muñoz, 2007; Pinyol and Alonso, 2010).

Geothermal piles are used to exchange heat from the ground for heating and cooling of superstructures (Brandl, 2006). In their cooling mode, the temperature of the circulated fluid is higher than the soil's temperature; hence, increasing the temperature of the latter. Under normal operating conditions the fluid can be up to 30 ^{o}C, although greater temperatures have been tested (e.g. Brandl, 2006; Bourne-Webb *et al*, 2009). In low permeability soils, these temperature increases have the potential to increase the pore water pressures and reduce the available effective stress. If this reduction is in the same order than the mobilised shaft friction, their effect on the shaft resistance can be significant.

In order to study the full thermo-hydro-mechanical interaction between pile and soil, Laloui *et al* (2006) presented the complete formulation of the problem and a solution compared to a field test. The excess pore water pressures are included implicitly within the formulation but since the values of permeability reported in their case study were in the order to 10^{-6} m/s, no significant excess pore water pressures were observed and remained constant. In turn, this had little effect on the available shaft friction. However, in the presence of lower permeability soils, these excess pore water pressures can reach values in the order of 1MPa for temperature increments of 30 ^{o}C (Munoz, 2007), which in most practical cases of bearing piles would exceed the effective stress at the interface.

Bourne-Webb *et al* (2009) presented another pile test with temperature cycling where they reported a difference of 15 kPa between the back-analysed – based on a mechanical test - shaft friction and the measured shaft friction.

Based on this evidence, this paper presents a finite difference solution to the fully coupled formulation to study the development of excess pore water pressures in geothermal piles and its impact on the shaft friction at the pile-soil interface. The emphasis will be on presenting comparisons in terms of orders of magnitude and not attempting to specify accurately all properties as this will change from case to case. The comparison does however, highlight an important issue that has been so far overlooked. The solution also provides a plausible explanation to the differences observed during the Lambeth College test presented in Bourne-Webb *et al* (2009).

Problem definition, assumptions and governing equations

Figure 1 shows the problem's geometry. A single pile diameter equal to 1m and pile length of 25m as used by Bourne-Webb *et al* (2009) were used. This length is enough to guarantee that seasonal effects are less important at mid-depth of the pile (Pasten & Santamarina, 2014) where the comparison between methods is carried out. In any case, as the problem is assumed to be one-dimensional for the purpose of this paper, the length is less critical.

The problem presents geometrical axisymmetry about the pile's axis so a cylindrical coordinate system (r,θ,z) was chosen as shown in Figure 1. Additionally, Loveridge & Powrie (2013, 2014) showed that the temperature difference at the pile surface for different positions within a pile diameter is lower than 2 ^{o}C: therefore, the azimuthal coordinate, θ, can be eliminated. Likewise, it is assumed that the temperature of the pile along its length is constant; this has been verified in site tests by multiple authors – e.g. Bourne-Webb *et al*. (2009), Laloui *et al*. (2006) for piles or Lee & Lam (2008) for boreholes. This, combined with an assumption of fully hydrostatic initial porewater profile, allows eliminating the z coordinate as well. The problem then becomes one dimensional, defined in the radial direction, r. It must be noted that this assumption is more representative of points distant from the ground surface where the temperature of the soils is subject to variations from above-ground effects. Hence, the comparisons between calculation methods – explained later – were done at mid-depth of the pile as indicated in Figure 1.

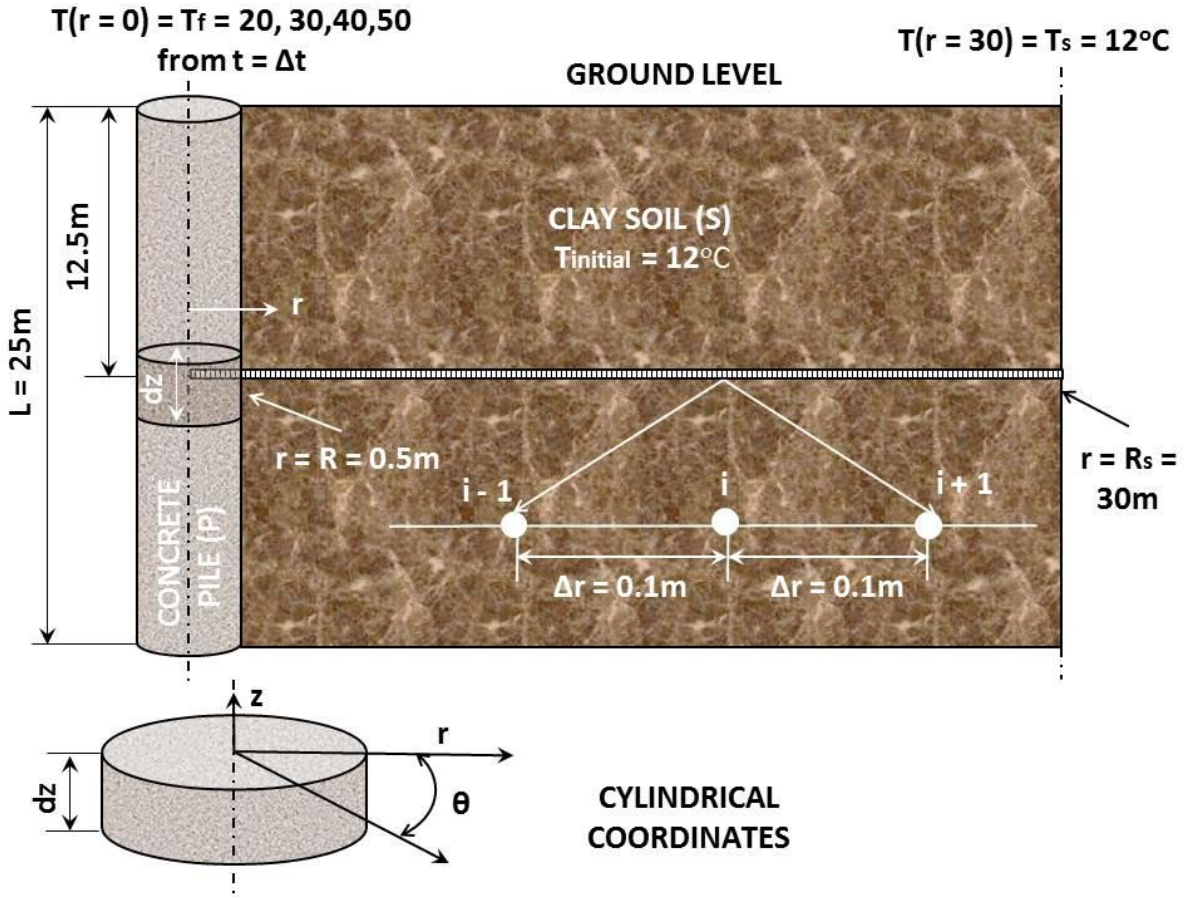

61

62 *Figure 1. Problem definition*

63 *Governing equations*

64 The thermo-hydro-mechanical formulation that defines the problem was presented generally by
65 Olivella *et al* (1996), and its application to piles by others like Laloui *et al* (2006). Both references
66 present the full equations derivation and therefore, this paper only presents the final equations. For
67 ease of reference, the reader is directed to Pinyol & Alonso (2010) as the same nomenclature has
68 been used here.

69 The heat equation for a constant thermal conductivity is

70 $$\frac{\partial T}{\partial t} = \alpha \frac{1}{r}\frac{\partial}{\partial r}\left(r\frac{\partial T}{\partial r}\right) = \alpha\left(\frac{1}{r}\frac{\partial T}{\partial r} + \frac{\partial^2 T}{\partial r^2}\right) \quad \text{Eq. 1}$$

71 where the convection effects have been ignored as demonstrated by Laloui *et al* (2006) for values of
72 permeability much higher than those covered here: hence, this assumption is even more applicable
73 to our case.

74 The combination of soil and water mass balance formulations yield the final governing second order
75 parabolic differential equation that applies only to the soil mass (Pinyol & Alonso, 2010)

$$-[(1-n)\beta_s + \beta_w n]\frac{\partial T_s}{\partial t} + \left(n\alpha_w + \frac{1}{K_s}\right)\frac{\partial u}{\partial t} - \frac{k}{\gamma_w}\frac{1}{r}\frac{\partial}{\partial r}\left(r\frac{\partial u}{\partial r}\right) = 0 \qquad \text{Eq. 2}$$

which has as unknowns the soil temperature, T_s, and the excess pore water pressures, u.

The main assumptions to derive the above equation are:

- The soil grains are incompressible against stress but not temperature changes.
- All the input variables – porosity, thermal conductivity, permeability, soil and water linear coefficients of thermal expansion, and soil and water compressibility - are independent of time, temperature and stress.
- The water table does not change throughout the test and therefore, in combination with small seepage forces due to low permeability, all changes to pore water pressures are due to the induced excess pore water pressures caused by thermal and mechanical strains.
- The soil volumetric deformation at the pile-soil interface can be characterised by a general one dimensional soil compressibility, K_S, as shown by Donna & Laloui (2014). The deformation caused in the pile due to temperature is therefore not included; however, notably, Di Donna & Laloui (2014) showed that the increment in horizontal stress at the pile-soil interface was only in the order of 5kPa due to temperature alone and therefore negligible.
- The total horizontal stress at the pile-soil interface remains constant.
- The plastic and long term effects at the pile-soil interface (Akrouch et al, 2014; Ng et al, 2014; Pasten & Santamarina, 2014; Stewart & McCartney, 2014; and Di Donna & Laloui, 2014) that arise as a consequence of multiple heating and cooling cycles have been ignored. A single heating cycle is considered here.

Most variables in equation 2 are well defined and show little variation in the context of thermal piles. Hence, only those where variations in practice can be present were selected to undertake the parametric study. These are: permeability, k, soil compressibility, K_S, and the temperature of the fluid, T_f. The influence of each of the three parameters, provided all others are fixed, is conceptually known: higher fluid temperature or compressibility and lower permeability, all produce greater excess pore water pressures. It is its extent that is investigated hereafter.

Table 1. Parameter values for the parametric study

Variable	Pile (C)	Soil particles (P)	Water (w)	Soil medium (S)
Porosity, n	-	-	-	0.25
Thermal expansion coefficient, β	-	3.00 E -05	3.42 E-04	1.10 E-04*

(1 / ^{o}C)				
Compressibility constant, water, α_w (1 / Pa)	-	-	5.00 E-10	-
Density, ρ (kg/m^3)	2,400	2,700	1,000	2,275*
Thermal conductivity, Γ (W/m^{o}C)	1.5	-	-	2.0
Specific heat, C (J /kg ^{o}C)	880.2	837.2	4,186	1,674.4*
Permeability, k (m/s)	-	-	-	1.00 E-8 1.00 E-9 1.00 E-10 1.00 E-11 1.00 E-12
Soil compressibility, K_S (Pa)	-	-	-	2.00 E06 2.00 E07 2.00 E08 2.00 E09 2.00 E10
Temperature of the fluid, T_f (ºC)	20 30 40 50	-	-	-

** These variables were calculated using the rule of mixes - e.g. for density, $\rho_s = \rho_P\ (1-n) + \rho_s\ n$.*

Table 1 presents the different values that have been used for the parametric study. The fluid temperature has been taken within the typical ranges of operation for geothermal foundations.

The range of permeability values used include those typical of low permeability clays like London Clay (Hight *et al*, 2007), Gault Clay (Ratman *et al*, 2005), Boom Clay (Horseman *et al*, 1980) or Opaline Clay (Thury *et al*, 2000). A maximum value of 1E-08 m/s was also used as an upper bound, beyond which Donna & Laloui (2014) demonstrated that induced excess porewater pressures are of no concern.

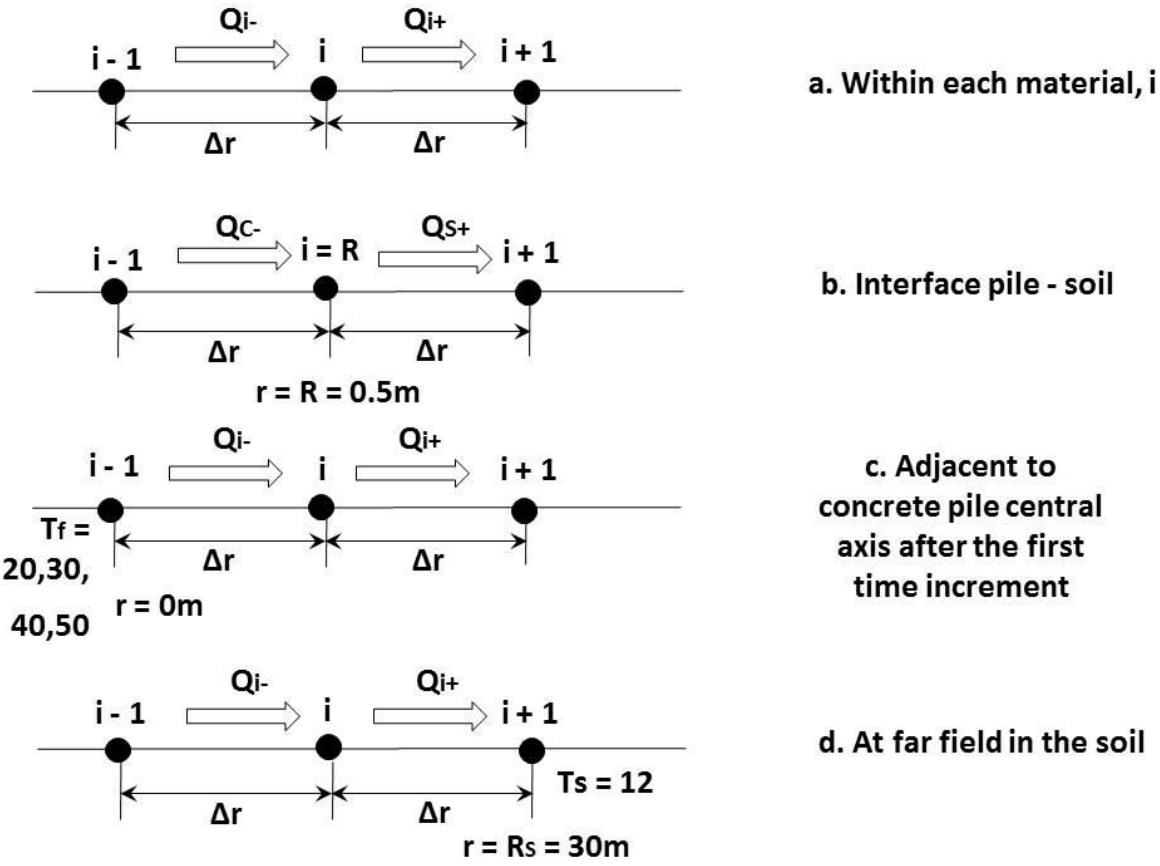

111

112 *Figure 2. Finite different discretization stencils*

113 **Analysis**

114 *Finite difference (FD)*

115 Equations 1 and 2 are uncoupled since the convective component caused by fluid movement
116 affecting the temperature has been ignored. Hence, equation 1 can be solved in isolation and the
117 results of this used as input into equation 2, which then turns into an equation where u is the only
118 unknown.

119 <u>Temperature field – Eq. 1</u>

120 The space domain was divided into three distinct stencils: within the pile, at the pile-soil interface,
121 and within the soil. The discretization was carried out using a regular grid size, Δr, of 0.0125m – see
122 Figure 2.

123 Developing the energy balance for points within each material yields

124 $$\Gamma_i(r_i - \Delta r/2)\frac{T_{i-1}-T_i}{\Delta r} - \Gamma_i\left(r_i + \frac{\Delta r}{2}\right)\frac{T_i-T_{i+1}}{\Delta r} = \rho_i C_i r_i \Delta r \frac{T_i'-T_i}{\Delta t}$$ Eq. 3

where the first term on the left hand side is the heat going into point i, Q_{i-}, and the second is the heat leaving point i, Q_{i+} - see Figure 2a. T_i' is the temperature in point i at the following time step. The right hand side of the equation is the heat generated in the vicinity of point i due to temperature changes in time. The equation can be rearranged to isolate T_i' as

$$T_i' = T_i + \alpha_i \frac{\Delta t}{r_i \Delta r^2}\left[\left(r_i - \frac{\Delta r}{2}\right)(T_{i-1} - T_i) - \left(r_i + \frac{\Delta r}{2}\right)(T_i - T_{i+1})\right] \quad \text{Eq. 4}$$

At the pile-soil interface, the problem involves both materials – see Figure 2b. The energy balance is as follows

$$\Gamma_c(R - \Delta r/2)\frac{T_{R-1} - T_R}{\Delta r} - \Gamma_s\left(R + \frac{\Delta r}{2}\right)\frac{T_R - T_{i+1}}{\Delta r} = (\rho_c C_c(R - \Delta r/4) + \rho_s C_s(R + \Delta r/4))\frac{\Delta r}{2}\frac{T_R' - T_R}{\Delta t}$$

Eq. 5

where T_R' is the temperature at the interface in the following time step. The terms are similar to those in equation 3. However, now the two different materials affect both the left and right hand side of the equations. Q_{i-} is Q_{c-} (within the concrete pile), and Q_{i+} is Q_{S+} (within the soil) – see Figure 2b.

T_R' can be then isolated as

$$T_R' = T_R + \frac{2\Delta t}{\Delta r^2}\frac{1}{(\rho_c C_c(R - \Delta r/4) + \rho_s C_s(R + \Delta r/4))}\left[\Gamma_c\left(R - \frac{\Delta r}{2}\right)(T_{R-1} - T_R) - \Gamma_s\left(R + \frac{\Delta r}{2}\right)(T_R - T_{R+1})\right]$$

Eq. 6

Two Dirichlet boundary conditions are used

$$T(r = 0) = T_f \quad \text{Eq. 7}$$

and

$$T(r = R_s) = T_s \text{ for any time, t} \quad \text{Eq. 8}$$

The initial conditions are constant temperature everywhere and equal to that of the soil

$$T = T_S \text{ for all points} \quad \text{Eq. 9}$$

In the first time increment, the temperature at the pile axis is then instantly increased to the fluid temperature – see Figure 2c.

The equation was solved explicitly in the time domain. An initial estimate of the maximum time step was calculated using the Neumman criteria for parabolic differential equations. For equation 1, this means

$$\Delta t_1 = \frac{\Delta r^2}{2\alpha_C} \quad \text{Eq. 10}$$

The consistency and stability of the solution was checked by using one order of magnitude lower than the calculated time step: if both yielded the same result, the solution was accepted. The same rationale was used to define the space discretization.

Excess pore water pressures field (soil only) – Eq. 2

Making

$$K_1 = -[(1-n)\beta_s + \beta_w n] \quad \text{Eq. 11}$$

$$K_2 = \left(n\alpha_w + \frac{1}{K_s}\right) \quad \text{Eq. 12}$$

$$K_3 = -\frac{k}{\gamma_w} \quad \text{Eq. 13}$$

allows rewriting eq. 2 as

$$K_1 \frac{\partial T_s}{\partial t} + K_2 \frac{\partial u}{\partial t} + K_3 \frac{\partial^2 u}{\partial r^2} = 0 \quad \text{Eq. 14}$$

The above equation was solved using the solver - function: ‘‘pdepe’’ - and the ordinary differential equation solver -function: ‘‘ode15s’’ - in MATLAB (version R2013b - 8.2.0.701).

A combination of Neumann,

$$\left(\frac{\partial u}{\partial r}\right)_{r=R} = 0 \quad \text{for any time, t} \quad \text{Eq. 15}$$

indicating that there is no flow at the pile-soil interface, and Dirichlet boundary conditions

$$u(r = R_s) = 0 \quad \text{for any time, t} \quad \text{Eq. 16}$$

that shows there is no excess porewater pressure generated in the far field.

The initial conditions are zero excess porewater pressures

$$u(t = 0) = 0 \quad \text{throughout} \quad \text{Eq. 17}$$

as it assumes a hydrostatic porewater pressure profile.

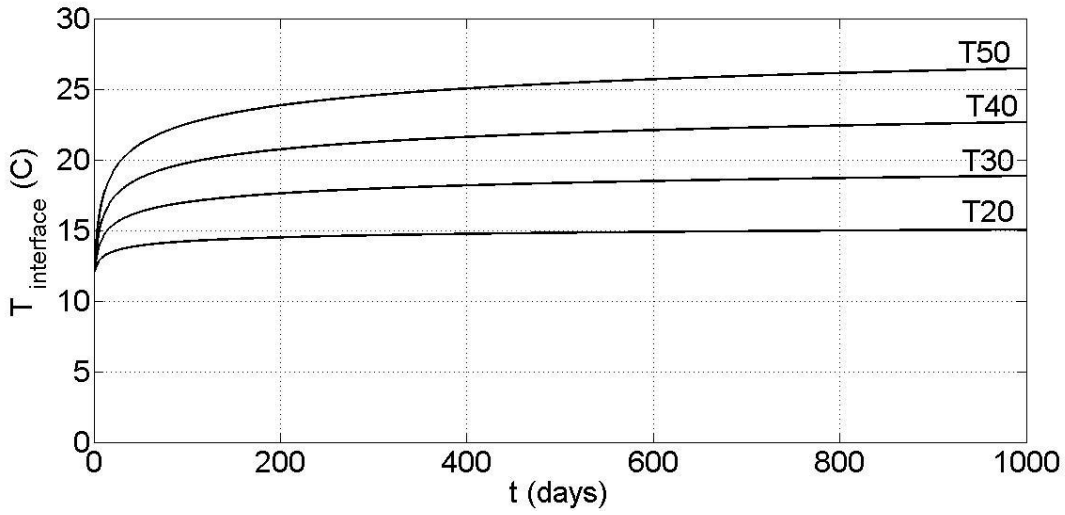

Figure 3. Temperature at the pile-soil interface vs time for the Tf values provided in Table 1.

Results and discussion

Figure 3 shows the different temperature profiles at the pile-soil interface evolving with time. A comparison is presented for the case of T_f = 30 °C. The FD solution converges towards a steady-state value just below 20 °C. This value was verified by calculating the steady state temperature obtained from Eq. 1 when removing the time dependant term with the same boundary and initial conditions.

Figure 4 shows the results of 100 models resulting from the combinations of T_f, k and K_s values shown in Table 1. As expected, lower permeability produce greater porewater pressures, as does a less compressible soil at the interface and obviously higher temperature. For the most detrimental combinations, the porewater pressure values reach over 0.2MPa, which is substantially higher than the available horizontal stress for typical geothermal piles.

Interestingly, increases of one order of magnitude in K_s result in much greater relative increments of excess porewater pressures than an order of magnitude decrement in permeability. This shows the importance of modelling the pile-soil interaction correctly and is shown by the greater slope in the K_s-u plane in Figure 4.

Shaft resistance reduction ratio

The importance of the presented induced excess porewater pressures can be expressed as a *shaft resistance reduction ratio* defined as

$$R_\tau = \frac{\tau_{w/temp}}{\tau_{wo/temp}} \qquad \text{Eq. 18}$$

where $\tau_{w/temp}$ is the shear at the pile-soil interface with temperature changes and $\tau_{wo/temp}$ without temperature.

But the shear at the interface can be generally written as

$$\tau = \sigma_h' \tan \varphi'$$

which can be developed into

$$\tau = K_m \sigma_v' \tan \varphi' \qquad \text{Eq. 19}$$

by using a mobilised earth pressure coefficient at the interface, K_m. Writing the vertical effective stress as a function of total and pore water pressures for the case with temperature gives

$$\tau_{w/temp} = K_m(\sigma_v - u_o - \Delta u) \tan \varphi' \qquad \text{Eq. 20}$$

where u_0 is the initial pore water pressure before temperature changes are applied, and Δu is the induced excess pore water pressure from temperature changes. The same can be done for the case without temperature as

$$\tau_{wo/temp} = K_m(\sigma_v - u_o) \tan \varphi' \qquad \text{Eq. 21}$$

Substituting Equations 20 and 21 into 18, and cancelling K_m and tan φ', gives the most general form of the shaft resistance reduction ratio

$$R_\tau = \frac{\sigma_v - u_o - \Delta u}{\sigma_v - u_o} \qquad \text{Eq. 22}$$

or

$$R_\tau = 1 - \frac{\Delta u}{\sigma_v - u_o} \qquad \text{Eq. 23}$$

The cancellation of the earth pressure coefficient and angle of shear resistance at the interface shown to write Eq. 22 can be done by assuming they do not change when the temperature gradient is applied. Since some authors like Di Donna & Laloui (2014) have shown that the strain and total stress changes at the interface are small when the temperature is applied, this assumption seems reasonable.

The ratio R_τ, is equal to 1.0 when there is no heat (i.e. $\Delta u = 0$), 0 if $\Delta u = \sigma_v - u_0$, and negative when $\Delta u > \sigma_v - u_0$, or in other words, when the excess porewater pressure is greater than the initial vertical effective stress.

For saturated soils where the water table is at the ground surface, $\sigma_v = \gamma_{sat} z$ and

220 $\gamma_{sat}z - u_0 = \gamma' z$, Eq. 22 can be rewritten as

221 $$R_\tau = 1 - \frac{\Delta u}{\gamma' z} \qquad \text{Eq. 24}$$

222 Similarly to Eq. 22, the ratio is equal to 1.0 when there is no heat (i.e. $\Delta u = 0$), 0 if $\Delta u = \gamma' z$, and
223 negative when $\Delta u > \gamma' z$.

224 For the purpose of this paper, it was assumed that the datum of *z* and the hydrostatic water table
225 are at ground level for simplicity. Based on this, we present the results at 10, 20, 30 and 40m depths
226 and the same combinations from Table 1 as previously, in Figure 5. It shows that, as expected, the
227 deeper the evaluation depth along the pile, the more safety is present. It also shows that for values
228 of permeability lower than 1.00 E-11 (m/s) and soil compressibility above 2E10 (Pa), the excess
229 porewater pressures exceed the available shaft resistance regardless of the depth – i.e. R_τ is lower
230 than 0. This highlights the importance of both values of k and K_s. Whilst, the temperature of the fluid
231 has an influence, this is much lower comparatively.

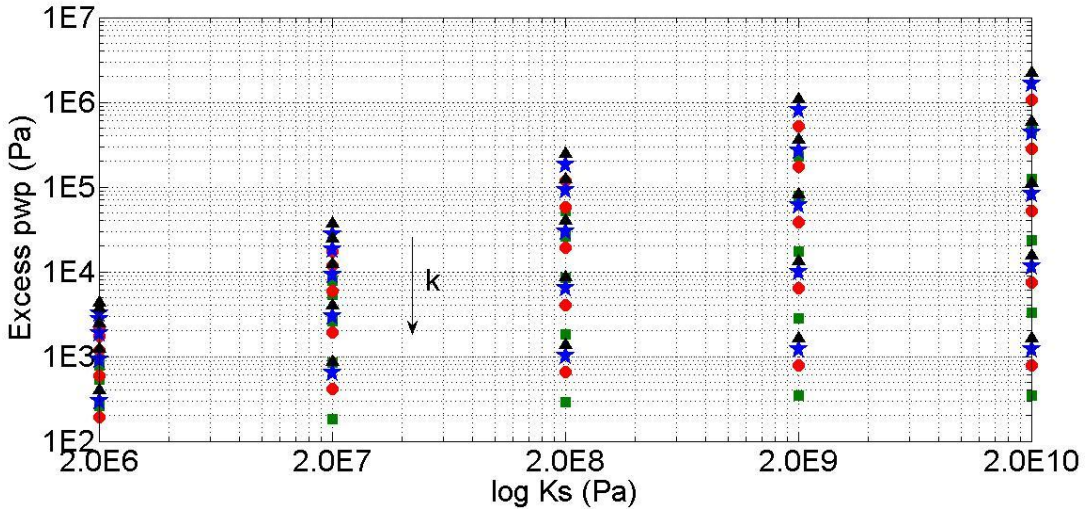

232

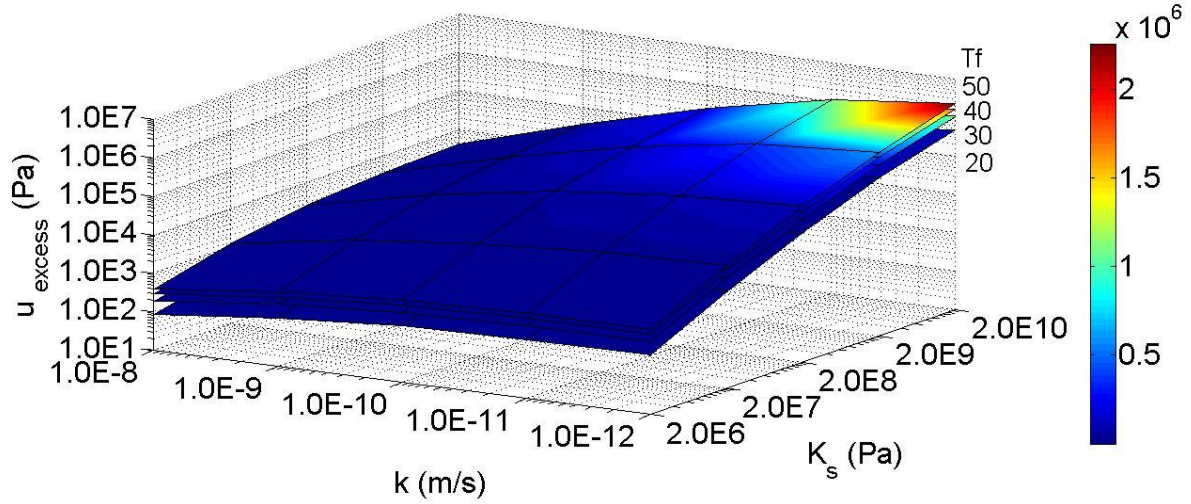

233

Figure 4. Calculated excess porewater pressures against: (a) Permeability, (b) Soil interface compressibility and (c) permeability and Soil interface compressibility – All axes are in logarithmic scale

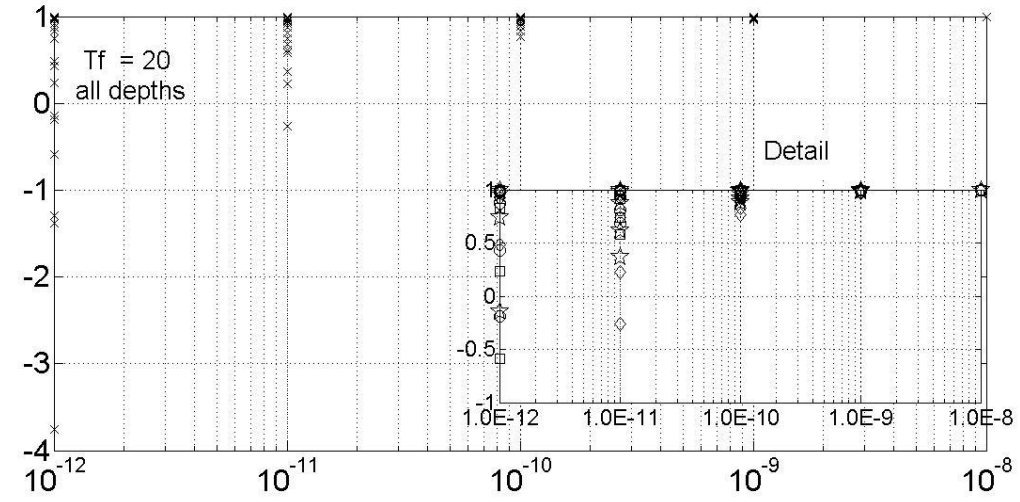

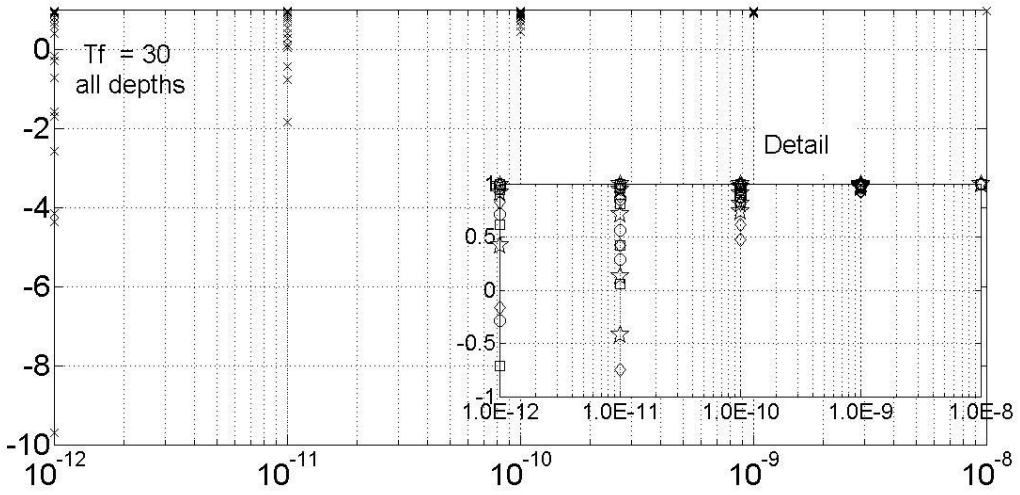

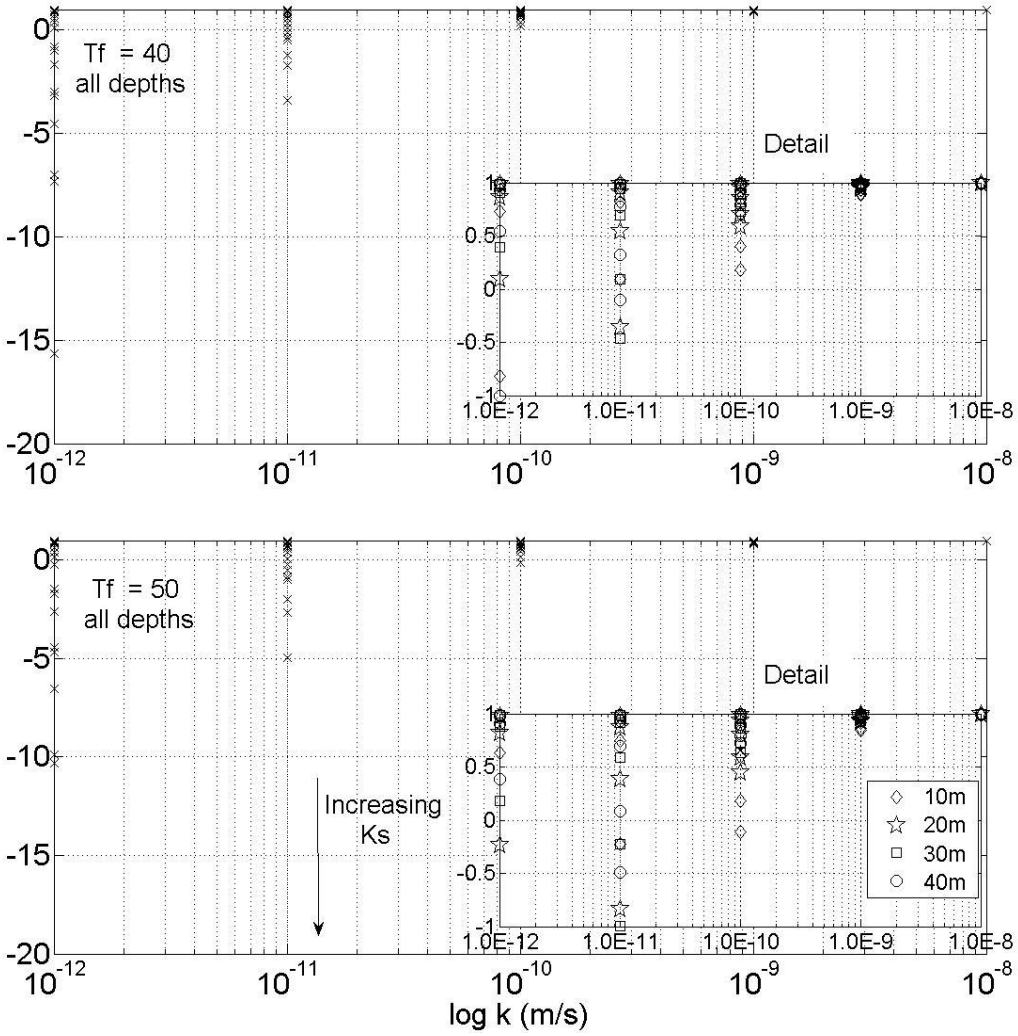

Figure 5. Shaft resistance reduction ratio vs permeability for different fluid temperatures: (a) 20°C , (b) 30°C, (c) 40°C, (d) 50°C.

Lambeth College test (Bourne-Webb et al, 2009) comparison

Figure 6 shows the results of the proposed semi-analytical FD solution to the case study of a test pile in London Clay presented by Bourne-Webb et al (2009). For the modelling, the temperature of the fluid, T_f, was taken as the temperature measurements in the pile presented by the authors. Values of permeability of 1E-9 m/s and 1E-10 m/s and soil compressibility equal to 3.71E10 Pa were taken from typical values presented by Hight et al (2007) for London Clay, as site specific measurements were not available.

The results in Figure 6 show that the temperature at the interface experiences small increments compared to the previous cases where the fluid temperature was sustained. Despite, the much lower values, it still shows an effect on the excess porewater pressures reaching values of 4 kPa and

31 kPa at the end of the first heating cycle for both values of permeability used. These values are comparable and provide upper and lower bounds to the unaccounted difference of 15kPa between the measured shaft friction and the ultimate shaft friction measured in the pile test Bourne-Webb et al (2009) reported. It therefore, provides a plausible explanation to this difference showing the effect of temperature on shaft friction.

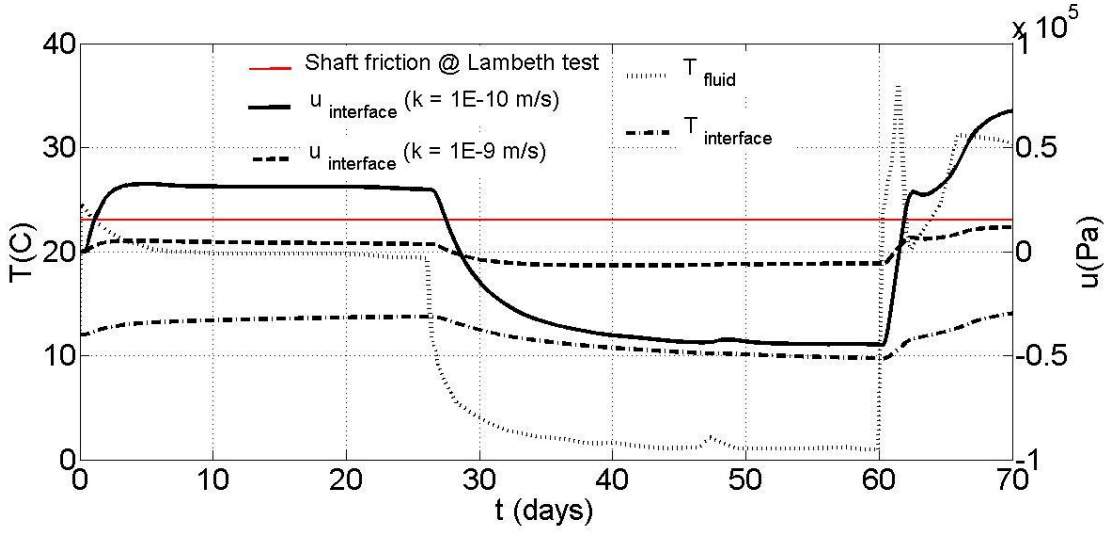

Figure 6. Temperature and excess porewater pressures for the Lambeth College case study.

Conclusions

The temperature induced excess pore water pressures in low permeability clays adjacent to thermal piles can be significant. Values in excess of 0.2MPa have been proven in this paper.

Soil permeability and soil compressibility are the most influential variables affecting the development of excess pore water pressures. In general, the lower the permeability, the greater the pore water pressure will be. Equally, for lower values of permeability the effect of the soil compressibility is accentuated, whereas in higher values of permeability, this is less relevant with regards to porewater pressures.

A new ratio named *shaft resistance reduction ratio* has been defined. It allows calculating, on a case by case basis, the potential for the developed pore water pressures to be of concern in terms of the shaft bearing capacity of thermal piles.

The parametric study has shown that only when the value of permeability is 1E-11 m/s or lower, combined with a soil compressibility in excess of 2E10 Pa, the excess porewater pressures were problematic. This combination of values of k and K_S are however characteristic of many overconsolidated clays.

The solution applied to the case of a test pile in London Clay, an overconsolidated clay, using typical values has provided a plausible explanation to the loss of shaft friction that was reported by Bourne-Webb *et al* (2009).

The results shown have significant implications for the design and operation of geothermal piles installed in low permeability and low compressibility soils and therefore, deserves further study from the community: the authors hope this paper will incentivise this. These effects are especially relevant in schemes were the ground is used as a heat sink for cooling during sustained periods of time. In more typical installations comprising heating and cooling cycles, the effect is smaller, but could also be comparably significant in relation to shaft friction resistance if the soil's permeability is very low.

Future work will focus on studying of the effect presented here with a more accurate pile-soil interaction modelling capable of modelling the plastic and long term deformations, concrete cracking, pile installation effects, and varying parameters with temperature and stress such as permeability and porosity.

References

Akrouch, G. A., Sanchez, M. & Briaud, J. (2014). Thermomechanical behavior of energy piles in high plasticity clays. *Acta Geotech*. **9**(3), 1–14.

Bourne-Webb, P. J., Amatya, B., Soga, K., Amis, T., Davidson, C., and Payne, P. (2009). Energy pile test at Lambeth College, London: Geotechnical and thermodynamic aspects of pile response to heat cycles. *Geotechnique*, **59**(3), 237–248.

Brandl, H. (2006). Energy foundations and other thermo-active ground structures. *Geotechnique*, **56**(2), 81–122.

Di Donna, A., and Laloui, L. (2014). Numerical analysis of the geotechnical behaviour of energy piles. *Int. J. Numer. Anal. Meth. Geomech*. **39**, 861–888.

Hight, D. W., Gasparre, A., Nishimura, S., Minh, N. A., Jardine, R. J. & Coop, M. R. (2007). Characteristics of the London Clay from the Terminal 5 site at Heathrow Airport. *Geotechnique* **57**(1), 3–18.

Horsemann S.T., Winter M.G., and Entwistle D.C., (1987). Geotechnical characterization of boom clay in relation to the disposal of radiactive waste. Commision Européenne.

Laloui, L. (2001). Thermo-mechanical behaviour of soils, *Revue Française de Génie Civil*, **5**(6), 809-843.

306 Laloui, L., Nuth, M., and Vulliet, L. (2006). Experimental and numerical investigations of the
307 behaviour of a heat exchanger pile. *Int. J. Numer. Anal. Meth. Geomech.*, **30**, 763–781.

308 Lee, C. K. and Lam, H. N. (2008). Computer simulation of borehole ground heat exchangers for
309 geothermal heat pump systems. *Renewable Energy*, **33**, 1286–1296.

310 Loveridge, F. and Powrie, W. (2014). 2D thermal resistance of pile heat exchangers. *Geothermics*, **50**,
311 122–135

312 Loveridge, F., Powrie, W. (2013). Pile heat exchangers: Thermal behaviour and interactions (2013)
313 *Proceedings of the Institution of Civil Engineers: Geotechnical Engineering*, **166** (2), 178-196

314 Munoz, J.J. (2007). Thermo-hydro-mechanical analysis of soft rock. Application to large scale heating
315 and ventilation tests. Doctoral thesis. Universitat Politecnica de Catalunya. Barcelona.

316 Ng, C. W. W., Shi, C., Gunawan, A. and LALOUI, L. (2014). Centrifuge modelling of energy piles
317 subjected to heating and cooling cycles in clay. *Geotechnique Letters* 4, 310–316,

318 Olivella, S., Gens, A., Carrera, J., Alonso, E.E. (1996). Numerical formulation for a simulator
319 (CODE_BRIGHT) for the coupled analysis of saline media. Engineering Computations 13 (7), 87-112.

320 Pasten, C. & Santamarina, J. C. (2014). Thermally induced long term displacement of thermoactive
321 piles. *J. Geotech. Geoenviron. Engng* **140**(5), 06014003.

322 Pinyol, N.M., Alonso, E.E.(2010). Fast planar slides. A closed-form thermo-hydro-mechanical
323 solution. *International Journal for Numerical and Analytical Methods in Geomechanics*, **34** (1), 27-52

324 Ratman, S., Soga, K. & Whittle, R. W. (2005). A field permeability measurement technique using a
325 conventional self-boring pressuremeter. *Geotechnique* **55**(7), 527–537.

326 Stewart, M. A., McCartney, J. S. (2014). Centrifuge Modeling of Soil-Structure Interaction in Energy
327 Foundations. *J. Geotech. Geoenviron. Eng.*, **140**(4).

328 Thury M., Boisson J.Y., and Bossar P., (2000). Le laboratoire souterrain du Mont Terri (Suisse) et
329 premiers résultats des études hydrogéologiques d'une formation argileuse. *Hydrogeologie*, **2,** 13-22.

330 Vardoulakis, I. (2002). Dynamic thermo-poro-mechanical analysis of catastrophic landslides.
331 *Geotechnique*, **52**(3), 157–171.

332

List of Figures

Figure 1. Problem definition

Figure 2. Finite different discretization stencils

Figure 3. Temperature at the pile-soil interface vs time for the Tf values provided in Table 1.

Figure 4. Calculated excess porewater pressures against: (a) Permeability, (b) Soil interface compressibility and (c) permeability and Soil interface compressibility – All axes are in logarithmic scale

Figure 5. Shaft resistance reduction ratio vs permeability for different fluid temperatures: (a) 20^{o}C , (b) 30^{o}C, (c) 40^{o}C, (d) 50^{o}C.

Figure 6. Temperature and excess porewater pressures for the Lambeth College case study.

342 **List of Tables**

343 *Table 1. Parameter values for the parametric study*